Advanced management of network overload in areas with Renewable Energies Sources

Thanh-Hung Pham * **Alessio Iovine** * **Sorin Olaru** *
Jean Maeght ** **Patrick Panciatici** ** **Manuel Ruiz** **

* *Laboratory of Signals and Systems (L2S), Centre National de la Recherche Scientifique (CNRS), CentraleSupélec, Paris-Saclay University, Gif-sur-Yvette, France*
{thanh-hung.pham,alessio.iovine,sorin.olaru}@centralesupelec.fr
** *Réseau de Transport d'Électricité (RTE), Paris, France*
{firstname.lastname}@rte-france.com

Abstract: This paper proposes an overload management method based on Model Predictive Control principles for electrical power network zones with Renewable Energies Sources (RESs). The danger of sudden line disconnection represents a critical aspect of the operation and the overload can only be tolerated within drastic duration and repetitiveness constraints. The first contribution resides in the employment of temporal and logical variables as a part of the system states to formulate supplementary bounds for the line power flow limits during the overload tolerance. For the second contribution, the control problem is independent from the exogenous overload trigger thanks to the feedback of these variables as the controller parameters. Lastly, according to considered assumptions, a sequence of predicted maximal supplementary bounds is used for the control design. With respect to classical additional temporal variables, these bounds simplify the control design problem. The proposed method is validated through simulations on an industrial study case.

Keywords: Power transmission network, constrained model predictive control, mixed logical dynamical modeling

1. INTRODUCTION

Due to the need to integrate renewable power, the power congestion management problem for electrical networks is increasing in complexity (see Meyer et al. (2020)). Indeed, the raising presence of renewable power multiplies the situations where the power production exceeds the maximum allowed power on the transmission lines, thus generating an overload (overcurrent). The overload induces an increase of conductor temperature, a conductor dilation which leads to a sag of the conductor which could create flashovers with the neighboring objects. The thermal phenomenon has an inertia, as described in Straub et al. (2018b), and the maximum current limits usually considered provide an aggregate admissible region for the current evolution. These limits are inherited from the time-domain evolution of the process and consequently the duration of the overload plays a critical role, associated here with a maximum allowed duration of constraint relaxation. Based on these principles, the overloads are temporarily tolerated, with strict limitations on their duration and repetitiveness. If the power excess is not admissible, the lines with power congestion may be disconnected from the network which possibly leads to a cascading lines tripping or blackouts (Monforti-Ferrario and Blanco (2021)).

One of the innovative approaches employed by Transmission System Operators (TSOs) to manage overloads and reduce their impact on the lines is related to the utilization of energy storage devices and renewable power curtailment through model-based optimization. As a consequence, approaches based on Model Predictive Control (MPC) can be used to design congestion management algorithms that target to limit the amount of power along the lines while ensuring problem feasibility and prioritizing the utilization of the available control actions (see Hoang et al. (2021)). A typical situation is depicted in Straub et al. (2018a) and Che et al. (2019), where the possibility to temporarily increase the maximal allowed power values is implemented by a change in the system of constraints handled by a MPC optimization algorithm. This MPC structure change was triggered by an independent supervisory mechanism, which was able to activate/deactivate the overload allowance and handle its duration by updating the constraints.

The goal of the present paper is to include the overload constraint updates within the MPC prediction mechanism. The MPC strategy will be based on an enhanced mathematical model and a set of state-dependent constraints. The solution does not rely on an exogenous decision making thus making the MPC mechanism self-consistent,

⋆ This work was carried out within the CPS4EU project, which has received funding from the ECSEL Joint Undertaking (JU) under grant agreement No 826276. The JU receives support from the European Union's Horizon 2020 research and innovation program and France, Spain, Hungary, Italy, Germany. The proposed results reflect only the authors' view. The JU is not responsible for any use that may be made of the information the present work contains.

differently from Straub et al. (2018a) where the optimisation problem resulted to have time-varying constraints depending on exogenous signals. To implement the rule-based adaptation of limitations, the adopted approach considers the utilization of logic variables as in Bemporad and Morari (1999), where the authors introduce a modeling framework for Mixed Logical Dynamical (MLD) systems that are composed by both real and logic variables and suggest MPC-based solutions for corresponding optimal control problems. The logic variables being defined via binary (or integer) variables, the control problems related to that modeling refer to mixed-integer programming. To investigate pros and cons of the possibility to consider a reduction of the number of binary variables, we avoid the formalism of Signal Temporal Logic (see Raman et al. (2014)), that usually implies the utilisation of tools that generate automatically the needed binary variables and are not customizable.

The proposed preliminary overload management controller is capable to adapt the power limitations to the current situation of the overload, thus imposing the end of the relaxation for the bounds in case the overload is over. Moreover, the controller is able to target to reduce the extra power on the lines according to selected power references, as according to a desired maximum overload duration. Finally, with or without overloads, the suggested MPC algorithm preserves the same structure. Indeed, in the considered modeling, temporal and logical variables are part of the system state, and describe the overload duration and the history of its tolerances. Their values carry the information needed to obtain a model-based control formulation that is independent of the unpredictable appearance of overloads. With respect to Straub et al. (2018a), the values of time-dependent constraints triggered by exogenous signals is replaced by a sequence of maximal predicted supplementary bounds for the power lines, thus facilitating the MPC formulation.

The paper is organized as follows. Section 2 recalls the MPC design in Hoang et al. (2021). Section 3 describes the control design for the overload management. Section 4 validates the method through simulations. Section 5 concludes the paper and presents future work directions.

2. CONGESTION MANAGEMENT VIA MPC

This section recalls the model and controller that are developed in Iovine et al. (2021) and Hoang et al. (2021), respectively, for the possibility to use a MPC-based approach that considers partial curtailment for congestion management of a power network zone, based on the concept of Power Transfer Distribution Factor (PTDF) in Cheng and Overbye (2005) (see Figure 2 for a zone example).

2.1 Modeling

Let n^N, n^C, n^B, $n^L \in \mathbb{N}$ denote the number of nodes in the considered zone, the number of nodes where the curtailment of the generated power is allowed, the number of nodes with a battery and the number of power lines in the zone, respectively. The state variables in a power network zone includes the line power flows, curtailment power, discharged battery power, battery energy, generated power and available renewable power which are denoted by $F(t) \in \mathbb{R}^{n^L}$, $P^C \in \mathbb{R}^{n^C}$, $P^B \in \mathbb{R}^{n^B}$, $E^B \in \mathbb{R}^{n^B}$, $P^G \in \mathbb{R}^{n^C}$ and $P^A \in \mathbb{R}^{n^C}$, respectively. The disturbance vector of the zone $w(t)$ gathers the generation power variation $\Delta P^G(t) \in \mathbb{R}^{n^C}$, the external interaction $\Delta P^T(t) \in \mathbb{R}^{n^L}$ and the available power variation $\Delta P^A(t) \in \mathbb{R}^{n^C}$, i.e., $w(t) = [\Delta P^T(t)\ \Delta P^G(t)\ \Delta P^A(t)]^\top \in \mathbb{R}^{n^N+2n^C}$. The variations of the curtailment power $\Delta P^C(t)$ and of the battery power $\Delta P^B(t)$ are chosen as the control vector $u(t)$, i.e., $u(t) = [\Delta P^C(t)\ \Delta P^B(t)]^\top \in \mathbb{R}^{n^C+n^B}$. Notice that the control actions are delayed with the operational time delays $d \geq 1$ and $\tau \geq 1$ for the battery power output and the generator power curtailment, respectively. The battery acts faster with respect to the renewable power curtailment, i.e., $\tau \geq d$. To deal with this known actuator delays, the system state vector $x(t)$ is defined as $x(t) = [F(t)\ P^C(t)\ P^B(t)\ E^B(t)\ P^G(t)\ P^A(t)\ \Delta P^C(t-\tau)\ \dots\ \Delta P^C(t-1)\ \Delta P^B(t-d)\ \dots\ \Delta P^B(t-1)]^\top \in \mathbb{R}^{n^L+(3+\tau)n^C+(2+d)n^B}$. Consequently, the resulting not-delayed system dynamics are:

$$x(t+1) = \tilde{A}x(t) + \tilde{B}u(t) + \tilde{D}w(t), \tag{1}$$

where the matrices $\tilde{A}$, $\tilde{B}$ and $\tilde{D}$ are:

$$\underbrace{\begin{pmatrix} A & B_C & \mathbf{0} & B_B & \mathbf{0} \\ \mathbf{0} & \mathbf{0} & \mathbf{I} & \mathbf{0} & \mathbf{0} \\ \mathbf{0} & \mathbf{0} & \mathbf{0} & \mathbf{0} & \mathbf{0} \\ \mathbf{0} & \mathbf{0} & \mathbf{0} & \mathbf{0} & \mathbf{I} \\ \mathbf{0} & \mathbf{0} & \mathbf{0} & \mathbf{0} & \mathbf{0} \end{pmatrix}}_{\tilde{A}}, \underbrace{\begin{pmatrix} \mathbf{0} & \mathbf{0} \\ \mathbf{0} & \mathbf{0} \\ \mathbf{I} & \mathbf{0} \\ \mathbf{0} & \mathbf{0} \\ \mathbf{0} & \mathbf{I} \end{pmatrix}}_{\tilde{B}}, \underbrace{\begin{pmatrix} D \\ \mathbf{0} \\ \mathbf{0} \\ \mathbf{0} \\ \mathbf{0} \end{pmatrix}}_{\tilde{D}}, \tag{2}$$

with the matrices A, B_C, B_B and D defined as:

$$\underbrace{\begin{pmatrix} \mathbf{I} & \mathbf{0} & \mathbf{0} & \mathbf{0} & \mathbf{0} & \mathbf{0} \\ \mathbf{0} & \mathbf{I} & \mathbf{0} & \mathbf{0} & \mathbf{0} & \mathbf{0} \\ \mathbf{0} & \mathbf{0} & \mathbf{I} & \mathbf{0} & \mathbf{0} & \mathbf{0} \\ \mathbf{0} & \mathbf{0} & -A_b & \mathbf{I} & \mathbf{0} & \mathbf{0} \\ \mathbf{0} & \mathbf{0} & \mathbf{0} & \mathbf{0} & \mathbf{I} & \mathbf{0} \\ \mathbf{0} & \mathbf{0} & \mathbf{0} & \mathbf{0} & \mathbf{0} & \mathbf{I} \end{pmatrix}}_{A}, \underbrace{\begin{pmatrix} M_t & M_c & \mathbf{0} \\ \mathbf{0} & \mathbf{0} & \mathbf{0} \\ \mathbf{0} & \mathbf{0} & \mathbf{0} \\ \mathbf{0} & \mathbf{I} & \mathbf{0} \\ \mathbf{0} & \mathbf{0} & \mathbf{I} \end{pmatrix}}_{D}, \underbrace{\begin{pmatrix} M_b \\ \mathbf{0} \\ \mathbf{I} \\ -A_b \\ \mathbf{0} \\ \mathbf{0} \end{pmatrix}}_{B_B}, \tag{3a}$$

$$B_C = \begin{pmatrix} -M_c & \mathbf{I} & \mathbf{0} & \mathbf{0} & -\mathbf{I} & \mathbf{0} \end{pmatrix}^\top. \tag{3b}$$

A_b, M_c, M_b and M_t are composed by the elements of the PTDF matrix as described in Iovine et al. (2021). The matrices $\mathbf{I}$ and $\mathbf{0}$ have appropriate dimensions with respect to the state x size, and to the delays τ and d. Particularly, the term $\Delta P^G(t)$ is defined as:

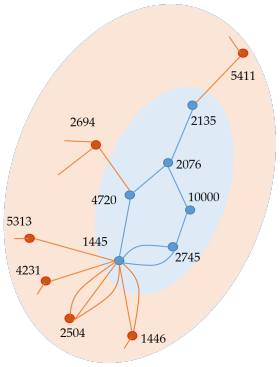

Fig. 1. The considered zone (blue nodes) and its neighborhood (red nodes) in Iovine et al. (2021).

$$\Delta P^G(t) = \min\left(f^G(t), g^G(t)\right), \tag{4a}$$
$$f^G(t) = P^A(t) + \Delta\hat{P}^A(t) - P^G(t) + \Delta\hat{P}^C(t-\tau), \tag{4b}$$
$$g^G(t) = \overline{P}^G - P^C(t) - P^G(t), \tag{4c}$$

where $\overline{P}^G \in \mathbb{R}_+^{n^C}$ is constant representing the maximum power that can be generated, $\Delta\hat{P}^A(t)$ and $\Delta\hat{P}^C(t-\tau)$ are pre-computed variables. The system model (1) is used for the control design in the next subsection.

2.2 Control design

Fig. 2 illustrates the control strategy, that is composed by forecasting, disturbance estimation, overload modeling and MPC. With respect to the strategy adopted in Hoang et al. (2021), the contribution of the present paper is highlighted in red, i.e. the overload modeling and related impact on the MPC strategy, and will be presented in the next section. In the sequel of the paper, the prediction horizon is N. Moreover, the predicted or estimated value of $g(.)$ at the sampling $t+k$ given the available information at the sampling t is denoted as $g(k|t)$.

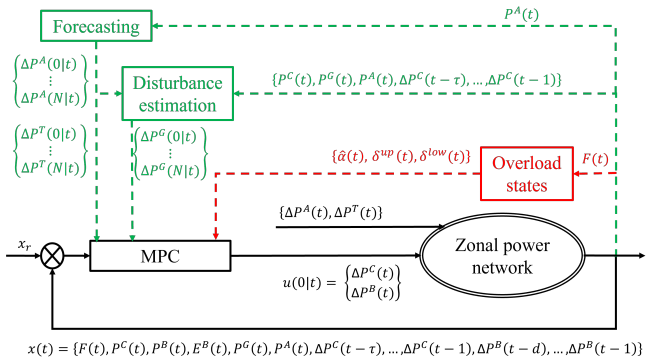

Fig. 2. Control scheme.

The *Forecasting* procedure predicts the variation of the available generator power $\Delta P^A(k|t)$ and the external interaction $\Delta P^T(k|t)$ over the prediction horizon. For robustness, the profile of $\Delta\hat{P}^A(k|t)$ is considered to be constant $\forall\ k \in [0, \ldots, N-1]$. In the same vein, there are multiple approaches for the prediction of $\Delta P^T(k|t)$. These choices can be integrated easily in the present control design. The performance of the disturbance estimation is not in the scope of the present work, and thus we will consider the simple one such as $\Delta P^T(k|t) = \mathbf{0}$.

The *Disturbance estimation* procedure evaluates the variation of the generated power $\Delta P^G(k|t)$ over the prediction horizon using the forecasting on $\Delta\hat{P}^A(k|t)$, the estimation of $\Delta\hat{P}^C(k|t)$ and (4). $\Delta P^C(k|t)$ will be given by the control design, and thus, the estimation is based on $\Delta\hat{P}^C(k|t) = \mathbf{0}$.

The *MPC* procedure determines the control signals $u(t)$ using the predicted disturbance sequences $w(k|t)$ and the state feedback $x(t)$. Let $\overline{L} \in \mathbb{R}_+^{n^L}$, $\overline{P}^G \in \mathbb{R}_+^{n^C}$, and $\overline{P}^B, \overline{E}^B \in \mathbb{R}_+^{n^B}$, denote the upper bounds of line power, generated power, battery power and battery energy, respectively; $\underline{P}^B \in \mathbb{R}_-^{n^B}$ and $\underline{E}^B \in \mathbb{R}_+^{n^B}$ denote the lower bounds of battery power and energy, respectively. To ensure the control problem feasibility, soft constraints are imposed to the flow on the power lines $F(k|t)$ for $k \in [d, \tau-1]$ using the softening slack variables $\varepsilon(k|t) \in \mathbb{R}^{n^L}$ such as $\varepsilon(k|t) > 0$, $\forall k \in [d, \tau-1]$, and $\varepsilon(k|t) = 0$, otherwise. Therefore, the constraints for the state x and for the control signal u are:

$$x_{min}(k|t) \leq Cx(k|t) \leq x_{max}(k|t),\ \forall k \in [d, N], \tag{5a}$$
$$u_{min} \leq u(k|t) \leq u_{max},\ \forall k \in [0, N-1], \tag{5b}$$

where $C = [\mathbf{I}_{n^L+2n^C+2n^B} \quad \mathbf{0}]$, and

$$x_{\min}(k|t) = [-\overline{L} - \varepsilon(k|t) \quad \mathbf{0} \quad \underline{P}^B \quad \underline{E}^B \quad \mathbf{0}]^\top, \tag{6a}$$
$$x_{\max}(k|t) = [\ \overline{L} + \varepsilon(k|t) \quad \overline{P}^G \quad \overline{P}^B \quad \overline{E}^B \quad \overline{P}^G]^\top, \tag{6b}$$
$$u_{min} = [\mathbf{0} \qquad \underline{P}^B - \overline{P}^B]^\top, \tag{6c}$$
$$u_{max} = [\overline{P}^G \qquad \overline{P}^B - \underline{P}^B]^\top. \tag{6d}$$

A cost function considering actuator delays is defined as:

$$J(t) = \sum_{k=1}^{N} \left[\|x(k|t) - x_r\|_Q^2 + \|u(k-1|t)\|_R^2 + \|\varepsilon(k|t)\|_\beta^2\right], \tag{7}$$

where Q and R are positive semi-definite matrices; β is a positive scalar; x_r is the state reference. Thus, the MPC optimization problem is defined as:

$$\mathcal{O}_0 = \underset{\{u(0|t),\ldots,u(N-1|t)\}}{\operatorname{argmin}} \quad J(t) \text{ in (7)}$$
$$s.t.\ (1), (5), (6). \tag{8}$$

Notice that an estimation of the disturbance $w(k|t)$ over the prediction horizon is proposed through two previous control procedures based on hypotheses about the available and curtailment power. Then, the first control actions $\Delta P^C(0|t)$ and $\Delta P^B(0|t)$ will be applied to the power networks at the instants $t+\tau$ and $t+d$, respectively.

3. OVERLOAD MANAGEMENT VIA MPC

This section firstly introduces additional state variables to describe the overload tolerance, and then, shows how they are integrated to the MPC design.

3.1 Additional states

Overloads in electrical power networks happen when the temperature of transmission lines exceeds predefined limits. These thermal limits are represented in this work by upper and lower bounds for the power flow on the lines. During the overload tolerance, non-negative supplementary bounds $\Delta_j^{up/low}(t)$ are used for the power flow on line j of the set $\mathcal{Z}^L$ of transmission lines in the zone. Hence, the alternative line power limits are described as:

$$-L_j - \Delta_j^{low}(t) - \varepsilon_j(t) \leq F_j(t) \leq L_j + \Delta_j^{up}(t) + \varepsilon_j(t), \tag{9}$$

where L_j, $\varepsilon_j(t)$ and $F_j(t)$ are the elements corresponding to the line j of the vectors $\overline{L}$, $\varepsilon(t)$ and $F(t)$ in (5)-(6d), respectively. Due to physical characteristics of the power line, $\Delta_j^{low}(t)$ and $\Delta_j^{up}(t)$ must be bounded when the overload happens at the instant t_o (see Fig. 5):

$$\Delta_j^{low/up}(t) \leq \begin{cases} \alpha_S,\ \forall t \in [t_o, t_o + T_{on}^S), \\ \alpha_L,\ \forall t \in [t_o + T_{on}^S, t_o + T_{on}^L), \\ 0,\ \text{else}, \end{cases} \tag{10}$$

where $\alpha_S,\ \alpha_L \in \mathbb{R}_+$, T_{on}^S and $T_{on}^L \in \mathbb{N}$ are thresholds determined from the operation of the real system with $0 < \alpha_L < \alpha_S$ and $0 < T_{on}^S < T_{on}^L$. The present paper considers the following assumptions:

(A1) on each line, only one of the upper and lower extra bound is allowed during an overload;
(A2) the time interval between two allowed overloads is greater than a predefined duration T_{off};
(A3) the overload is not predictable;
(A4) in the MPC formulation, as soon as the overload is over, its tolerance is ended;
(A5) if there is no feasible solution for the control law, the overloaded line is opened;
(A6) the maximal supplementary bounds defined in (10) are used until the overload is over.

For mathematical modeling purposes, a temporal variable $t_j^a(t) \in \mathbb{N}$ is added to the system states for representing the overload duration, and thus, indicating the maximal value of supplementary bounds in (10) to be taken into account at each time instant. It is zero during the normal operation, and linearly increases during the overload. On the other hand, two logical variables $\delta_j^{up}(t)$ and $\delta_j^{low}(t)$ are added to the system states to manage the overload moments. They are equal to 1 if and only if the overload is admissible or the supplementary bounds are positive. Hence, the dynamics of $t_j^a(t)\ \forall j \in \mathcal{Z}^L$ is given as:

$$t_j^a(t) = \left[t_j^a(t-1)+1\right]\left[\delta_j^{up}(t-1)+\delta_j^{low}(t-1)\right]. \quad (11)$$

An overload is admissible only in two following cases:

- Case 1: the overload tolerance is activated at the current time, i.e., $\delta_j^{up/low}(t-1)=0$ and $F_j(t) > L_j$ (or $F_j(t) < -L_j$), and the previous overload happened long time ago, i.e., $\sum_{i=1}^{T_{off}}\left[\delta_j^{up}(t-i)+\delta_j^{low}(t-i)\right]=0$.
- Case 2: the overload is happening, i.e., $\delta_j^{up/low}(t-1)=1$ and $F_j(t) > L_j$ (or $F_j(t) < -L_j$), and it is still admissible, i.e., $t_j^a(t) \le T_{on}^L - 1$.

Consequently, the dynamics of $\delta_j^{up/low}(t)$ are given as:

$$\delta_j^{up/low}(t)=1 \Leftrightarrow \left[\begin{array}{l} \left\{\begin{array}{l} \underbrace{F_j(t) \ge L_j+\gamma}_{up}\ (or\ \underbrace{F_j(t) \le -L_j-\gamma}_{low}), \\ \sum_{i=1}^{T_{off}} \delta_j^{up}(t-i)+\delta_j^{low}(t-i)=0, \end{array}\right. \\ \left\{\begin{array}{l} \underbrace{F_j(t) \ge L_j+\gamma}_{up}\ (or\ \underbrace{F_j(t) \le -L_j-\gamma}_{low}), \\ \delta_j^{up/low}(t-1)=1, \\ t_j^a(t) \le T_{on}^L-1. \end{array}\right. \end{array}\right. \quad (12)$$

$\forall j \in \mathcal{Z}^L$, where $\gamma \in \mathbb{R}$ is a small tolerance value. According to Assumption (A6), the supplementary bounds $\Delta_j^{up/low}$ in (9) are formulated as:

$$\Delta_j^{up/low}(t) = \alpha\left(t_j^a(t)\right)\delta_j^{up/low}(t),\ \forall j \in \mathcal{Z}^L. \quad (13)$$

where $\alpha\left(t_j^a(t)\right)$ is predefined as:

$$\alpha\left(t_j^a(t)\right) = \left\{\begin{array}{ll} \alpha_S, & \text{if } 0 \le t_j^a < T_{on}^S, \\ \alpha_L, & \text{if } T_{on}^S \le t_j^a < T_{on}^L, \\ 0, & \text{else.} \end{array}\right. \quad (14)$$

3.2 Feedback policy

An implementation in the MPC formulation of the additional state dynamics and of the supplementary bounds defined in (11)-(14) requires a complex MLD modelling. Fortunately, we show through the following proposition that this complexity can be simplified.

Proposition 1. If the Assumptions (A1), (A3), (A4) and (A5) are respected, the implementation of (11)-(13) in the MPC design is for all k equivalent to:

$$\delta_j^{up/low}(k|t)=1 \Leftrightarrow \left\{\begin{array}{l} \underbrace{F_j(k|t) \ge L_j+\gamma}_{up}\ (or\ \underbrace{F_j(k|t) \le -L_j-\gamma}_{low}) \\ \delta_j^{up/low}(k-1|t)=1 \end{array}\right., \quad (15)$$

$$\Delta_j^{up/low}(k|t) = \alpha(t_j^a(0|t)+k)\ \delta_j^{up/low}(k|t). \quad (16)$$

Proof. i) [(15)] First, (A3) and (A4) imply that:

$$\delta_j^{up/low}(k|t) \le \delta_j^{up/low}(k-1|t),\ \forall k \in [1,N]. \quad (17)$$

Moreover, the temporal constraint $t_j^a(k|t) \le T_{on}^L - 1$ is not necessary since it is implicitly defined in the formulation of α in (14) with the constraints (9) and (13). Therefore, from (12) and (17), we obtain the simplified dynamics of $\delta_j^{up/low}(k|t)$ in (15). Notice that this is not the case for the real system, where (11)-(12) are applied, since the values of $\delta^{up/low}(t)$ are not influenced by $\alpha(t)$.

ii) [(16)] If $\delta_j^{up/low}(k|t) = 0$, (16) trivially holds. If $\delta_j^{up/low}(k|t) = 1$, $\delta_j^{up/low}(j|t) = 1$, $\forall j \in [0,\dots,k]$, and $\delta_j^{low/up}(k|t)=0$, $\forall k \in [0,\dots,N]$ thanks to (17) and (A1). Hence, $t_a(k|t) = t_a(0|t)+k$ according to (11), and thus, (16) holds. Consequently, the explicit description of the dynamics of $t_a(t)$ in (11) is not necessary anymore within the prediction mechanism of the MPC. □

With respect to (12), the dynamics (15) are much simpler. Moreover, from (16), instead of the temporal state feedback $t_j^a(t)$ with the complex formulations defined in (11) and (13)-(14), a sequence $\hat{\alpha}_j(t)$ gathers $N+1$ predicted maximal supplementary bounds over the prediction horizon computed from $t_j^a(t)$ and (14) is used in the MPC design Finally, the current values of the logical state variables $\delta_j^{up/low}(t)$ and the prediction sequence $\hat{\alpha}_j(t)$ are fed to the MPC controller as described in Fig. 2.

3.3 Modified MPC design

To gather the logical variables and supplementary bounds for all lines in the zone, we denote $\delta^{up/low} = col\left[\delta_j^{up/low}\right]$, $\Delta^{up/low} = col\left[\Delta_j^{up/low}\right]$, $\forall j \in \mathcal{Z}^L$. Hence, the dynamics of $\delta^{up/low}(k|t)$ in (15) are described using the big-M reformulation (Bemporad and Morari (1999)) as:

$$\begin{aligned} -M_\delta \delta^{up}(k|t) &\le \overline{L}+\gamma\mathbf{1}-F(k|t)+M_x(\mathbf{1}-\delta^{up}(k-1|t)) \\ &\le M_\delta(\mathbf{1}-\delta^{up}(k|t)),\ \forall k \in [1,N], \quad (18a) \\ -M_\delta \delta^{low}(k|t) &\le \overline{L}+\gamma\mathbf{1}+F(k|t)+M_x(\mathbf{1}-\delta^{low}(k-1|t)) \\ &\le M_\delta(\mathbf{1}-\delta^{low}(k|t)),\ \forall k \in [1,N], \quad (18b) \end{aligned}$$

respectively, where M_x and M_δ are sufficiently large numbers. Based on (9) and (16), the limits (6a)-(6b) are modified as:

$$x_{\min}(k|t) = [-\overline{L}-\Delta^{low}(k|t)-\varepsilon(k|t)\ \mathbf{0}\ \underline{P}^B\ \underline{E}^B\ \mathbf{0}]^\top, \quad (19a)$$

$$x_{\max}(k|t) = [\ \overline{L}+\Delta^{up}(k|t)+\varepsilon(k|t)\ \overline{P}^G\ \overline{P}^B\ \overline{E}^B\ \overline{P}^G]^\top. \quad (19b)$$

Finally, the optimization problem (8) is modified such as:

$$\mathcal{O}_1 = \underset{\{u(0|t),\ldots,u(N-1|t)\}}{\operatorname{argmin}} \quad J(t) \text{ in (7)}$$
$$s.t.\ (1),(5),(6c),(6d),(16),(18),(19). \tag{20}$$

The presented control design will be validated through simulations on a specific study case of industrial interest.

3.4 Discussion

This subsection addresses two possible improvements for the presented MPC formulation (20):

- reduction of the number of binary variables,
- early and soft decision of the generators curtailment.

The first objective can be achieved by assuming that the overload is admissible over the prediction horizon if it is currently admissible, i.e., $\delta_j^{up/low}(k|t) = \delta_j^{up/low}(0|t)$. This also implies that multiple overloads are allowed in the MPC formulation, and thus, the assumption (A4) is relaxed. Therefore, the constraints (18) are not necessary, and the supplementary bounds in (16) are modified as:

$$\Delta_j^{up/low}(k|t) = \alpha(t_j^a(0|t) + k)\ \delta_j^{up/low}(t),\ \forall j. \tag{21}$$

The resulted MPC optimization problem is defined as:

$$\mathcal{O}_2 = \underset{\{u(0|t),\ldots,u(N-1|t)\}}{\operatorname{argmin}} \quad J(t) \text{ in (7)}$$
$$s.t.\ (1),(5),(6c),(6d),(19),(21). \tag{22}$$

Consequently, the number of binary variables of $\mathcal{O}_2$ in (22) is N times smaller with respect to $\mathcal{O}_1$ in (20), and $4n^L N$ constraints in (18) are eliminated. However, this control design reduces the control effort to deal with the overload.

On the other hand, in (20), the curtailment decision is postponed as late as possible with sudden and great variations. To obtain an early and soft decision, we can penalize in the cost function (7) the surplus amount of line power flows during the overload such that:

$$J_3(t) = J(t) + \phi \sum_{k=1}^{N} \Big[\left(C_3 x(k|t) - \overline{L}\right)^\top \delta^{up}(k|t) + \left(-C_3 x(k|t) - \overline{L}\right)^\top \delta^{low}(k|t) \Big], \tag{23}$$

where $C_3 = [\mathbf{I}_{n^L}\ \mathbf{0}]$, $\phi \in \mathbb{R}$ is a chosen weight. Thus, the corresponding MPC optimization problem is defined as:

$$\mathcal{O}_3 = \underset{\{u(0|t),\ldots,u(N-1|t)\}}{\operatorname{argmin}} \quad J_3(t) \text{ in (23)}$$
$$s.t.\ (1),(5),(6c),(6d),(16),(18),(19). \tag{24}$$

This nonlinearity in the cost function can be solved using numerical optimization toolboxes, but increases the complexity of the optimization problem. Moreover, the curtailment moment is sensitive to the choice of ϕ.

4. SIMULATIONS

This section presents closed-loop simulations for a zone of power networks which has six nodes, seven lines, four generators and one battery, as illustrated in Fig. 2. The parameters of zone model, control algorithm and simulations are presented in Table 1. The simulations are implemented in MATLAB; the control algorithms are programmed by using YALMIP in Löfberg (2004); the MPC optimization problems are solved by using GUROBI solver in Gurobi Optimization (2021). A suitable value of M_δ in (18) is chosen using the function *implies* in YALMIP.

Table 1. Parameters.

Parameter	Value
Number of nodes n^N and of lines n^L	6 and 7
Number of curtailed generators n^C	4
Number of batteries n^B	1
Line power limit L_j [MW]	45
Generators power limits $\bar{P}^G$ [MW]	$[78\ 66\ 54\ 10]^\top$
Battery power limits $[\underline{P}^B\ \bar{P}^B]$ [MW]	[-10 10]
Battery delay d [s]	5
Curtailment actuator delay τ [s]	35
Extra bound amplitudes α_S and α_L [MW]	45 and 20
Extra bound durations T_{on}^S and T_{on}^L [s]	120 and 360
Two overloads' interval T_{off} [h]	12
Prediction horizon N	10
State weight matrix Q	$diag\{\mathbf{0}_{7\times7}\ \ \mathbf{I}_4\ \ 10^{-3}\ \ \mathbf{0}_{34\times34}\}$
Input weight matrix R	$\mathbf{I}_5$
Parameter M_x [MW] in (18)	200
Sampling time T [s]	5
Simulation time [s]	600

Three simulation Scenarios are considered, where the three optimisation problems $\mathcal{O}_1$ in (20), $\mathcal{O}_2$ in (22), and $\mathcal{O}_3$ in (24) are implemented via MPC. With the MPC design $\mathcal{O}_0$ in (8), a violent curtailment of renewable power is decided as soon as the overload appears (see Hoang et al. (2021) for more details), which is not the case of the present work. The real power transmission network is emulated in these simulations through the implementation of the function *runpf* in MATPOWER toolbox for the whole French transmission network including around 6000 buses (Josz et al. (2016)). During the simulations, two independent disturbances are directly injected into the lines (1445,2745) and (2076,2135) (see Fig. 2) as:

$$\eta_1(t) = \begin{cases} 30\ [MW], \text{ if } t \geq 30s, \\ 0\ [MW], \text{ else,} \end{cases} \tag{25a}$$

$$\eta_4(t) = \begin{cases} -30\ [MW], \text{ if } 300s \leq t \leq 350s, \\ 0\ [MW], \text{ else.} \end{cases} \tag{25b}$$

With respect to the first scenario describing problem $\mathcal{O}_1$ in (20), Fig. 3 illustrates the curtailment power variations. We see that the generator power is not curtailed when the overload happens at $t = 50s$ on the line 1. The curtailment is postponed until $t = 135s$, i.e., $\tau = 35s$ before the smaller extra bound for this line power flow is applied at $t = 170s$ (see Fig. 4). At $t = 375s$, the curtailment is decided for the application at $t = 410s$ because the overload on the line (1445,2745) will not be allowed from $t = 410s$.

In scenario 2 related to problem $\mathcal{O}_2$ in (22), Fig. 5 illustrates the power flow profile of line 1. In principle, it shows that the control law leads to the same curtailment policy obtained by $\mathcal{O}_1$ in (20) (Fig. 4). However, this similarity in the closed-loop behaviour may not be generally true and the equivalence conditions deserve further study.

In Scenario 3 corresponding to problem $\mathcal{O}_3$ in (24), Fig. 6 illustrates the power flow profile of line 1. We can see that the generator power is softly curtailed with a delay of $\tau = 35s$ after the overload appearance. The first remark for the parameter tuning is that the input weight R and the additional term weight ϕ must be of the same amplitude

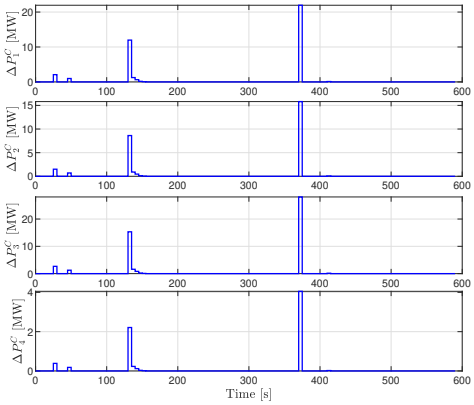

Fig. 3. Curtailment power variation in Scenario 1.

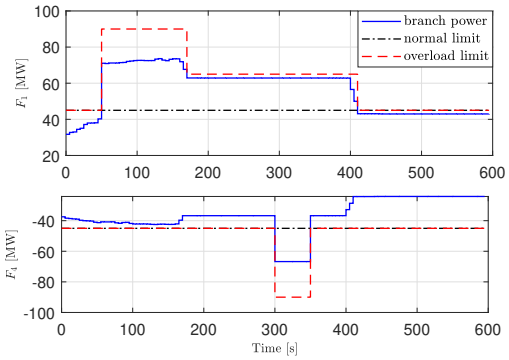

Fig. 4. Power flows of lines 1 (upper) and 4 (lower) in Scenario 1.

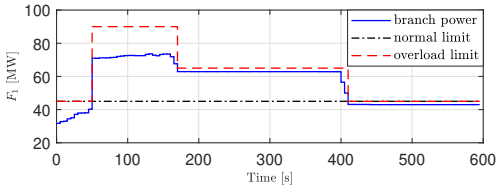

Fig. 5. Power flow of line 1 in Scenario 2.

order. Another remark indicates that to increase these weight reduces the overload duration.

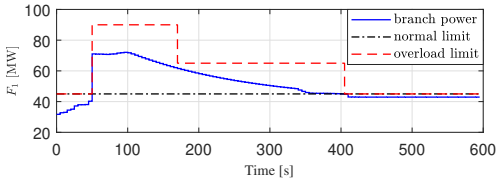

Fig. 6. Power flow of line 1 in Scenario 3 with $R = 10^2\mathbf{I}_5$ and $\phi = 3 \times 10^2$.

5. CONCLUSIONS

This paper proposed an approach for overload management in transmission power networks via MPC with a model composed of both real and logical variables. The resulting mixed-integer optimisation problem is independent of the exogenous overload trigger, and therefore does not suffer of feasibility problems. Moreover, the proposed approach deals with the unfortunate event of having multiple overloads. Important aspects as reduction of the number of binary variables or the possibility to partially act on the overload during the transient time are considered in two other optimisation problems, based on the same modeling. The proposed method has been validated through simulations on an industrial study case. The short term future work focuses on a linear modeling of the renewable generator power using the signal temporal logic formulation.

REFERENCES

Bemporad, A. and Morari, M. (1999). Control of systems integrating logic, dynamics, and constraints. *Automatica*, 35(3), 407–427.

Che, L., Liu, X., and Shuai, Z. (2019). Optimal transmission overloads mitigation following disturbances in power systems. *IEEE Transactions on Industrial Informatics*, 15(5), 2592 – 2604.

Cheng, X. and Overbye, T. (2005). PTDF-based power system equivalents. *IEEE Transactions on Power Systems*, 20(4), 1868–1876.

Gurobi Optimization, L. (2021). Gurobi optimizer reference manual. URL `http://www.gurobi.com`.

Hoang, D.T., Olaru, S., Iovine, A., Maeght, J., Panciatici, P., and Ruiz, M. (2021). Power Congestion Management of a sub-Transmission Area Power Network using Partial Renewable Power Curtailment via MPC. In *Control and Decision Conference (to appear). (hal-03405213)*.

Iovine, A., Hoang, D.T., Olaru, S., Maeght, J., Panciatici, P., and Ruiz, M. (2021). Modeling the partial renewable power curtailment for transmission network management. In *2021 IEEE Madrid PowerTech*, 1–6.

Josz, C., Fliscounakis, S., Maeght, J., and Panciatici, P. (2016). AC power flow data in MATPOWER and QCQP format: itesla, RTE snapshots, and PEGASE. *arXiv:1603.01533*.

Löfberg, J. (2004). Yalmip : A toolbox for modeling and optimization in matlab. In *In Proceedings of the CACSD Conference*. Taipei, Taiwan.

Meyer, B., Astic, J., Meyer, P., Sardou, F., Poumarede, C., Couturier, N., Fontaine, M., Lemaitre, C., Maeght, J., and Straub, C. (2020). Power Transmission Technologies and Solutions: The Latest Advances at RTE, the French Transmission System Operator. *IEEE Power and Energy Magazine*, 18(2), 43–52.

Monforti-Ferrario, F. and Blanco, M.P. (2021). The impact of power network congestion, its consequences and mitigation measures on air pollutants and greenhouse gases emissions. A case from Germany. *Renewable and Sustainable Energy Reviews*, 150, 111501.

Raman, V., Donzé, A., Maasoumy, M., Murray, R.M., Sangiovanni-Vincentelli, A., and Seshia, S.A. (2014). Model predictive control with signal temporal logic specifications. In *53rd IEEE Conference on Decision and Control*, 81–87.

Straub, C., Olaru, S., Maeght, J., and Panciatici, P. (2018a). Zonal Congestion Management Mixing Large Battery Storage Systems and Generation Curtailment. In *2018 IEEE Conference on Control Technology and Applications (CCTA)*, 988–995.

Straub, C., Olaru, S., Maeght, J., and Panciatici, P. (2018b). Robust MPC for temperature management on electrical transmission lines. *IFAC-PapersOnLine*, 51(32), 355–360. 17th IFAC Workshop on Control Applications of Optimization CAO 2018.